Acta Cryst. (1988). A44, 374-379

Extinction in Time-of-Flight Neutron Powder Diffractometry

BY T. M. SABINE

NSW Institute of Technology, Sydney, NSW 2007, *Australia*

R. B. VON DREELE

*LANSCE, MS H*805, *Los Alamos National Laboratory, Los Alamos, NM* 27545, *USA*

AND J.-E. JØRGENSEN

The Studsvik Neutron Research Laboratory, S-611 *Nyköping, Sweden*

(*Received* 14 *September* 1987; *accepted* 15 *January* 1988)

Abstract

Time-of-flight data have been collected from polycrystalline specimens of magnesium oxide in which the grain size distribution is known. These data were obtained at scattering angles of 150, 90 and 60°. A primary extinction factor given in an analytical form by Sabine [*Acta Cryst.* (1988), A44, 368-373] is included in a Rietveld program. The experimental data from the two high-angle histograms are refined to give an effective mosaic block size and overall temperature factors. The effective mosaic block size is used in the calculation of an extinction factor for each reflection. This factor is then compared with the ratio of measured integrated intensities. The theoretical form of the extinction factor is verified to a level of 0·30. The temperature factors measured from each specimen are identical and in agreement with the best literature value.

1. Introduction

A well known problem in the analysis of time-of-flight (TOF) data by the Rietveld method (Rietveld, 1969) has been an inability to extract consistent temperature factors, when analyses are made of data on the same specimen taken over different ranges in TOF. In most cases the temperature factors from the complete data set are low and in some cases negative. As the upper TOF bound of the data is made shorter the values of the apparent temperature factor rise.

This problem is caused by primary extinction within each perfect crystal block in the powder. In a brittle material the block size may be equal to the grain size; in a ductile material the block size may be orders of magnitude smaller than the grain size and may coincide with the sub-grain size.

Extinction is dependent on both wavelength and scattering angle. However, the large range of wavelengths used in TOF experiments makes the problem more obvious. In both techniques the measured temperature factors have lower values than the true temperature factors.

A factor which can be used to correct integrated intensities for the effect of primary extinction has been derived by Sabine (1985, 1988). The first experimental tests of the validity of that factor were carried out by neutron measurements on polycrystalline specimens of magnesium oxide using a constant wavelength.

An attempt was made to arrange the experiment so that there were no disposable parameters. The only crystallographic parameters for MgO are the Debye-Waller factors for each atom. Values found for these have been reviewed in detail by Barron (1977).

The shape of the grains and the grain size distribution in each specimen were determined by scanning electron microscopy. An untested assumption was that each grain was a perfect crystal.

In the present experiment time-of-flight methods are used on the same specimens to provide a more stringent test of the theory. TOF measurements have the advantage of a larger range of $(\sin\theta)/\lambda$, and a direct method of scaling data collected from specimens of different mass.

Four sets of TOF data are analysed by the Rietveld computer program of Larson & Von Dreele (1986) to give an overall temperature factor and an average mosaic block size. The block size is compared with direct measurements of the extinction factors and the temperature factor is compared with literature values.

2. Magnesium oxide

Magnesium oxide has the rock salt structure. The space group is O_h^5-$Fm\bar{3}m$ (No. 225); a = 4·21145 (3) Å (Howard & Sabine, 1974). The Mg and O atoms are located at 0, 0, 0 and $\frac{1}{2}, \frac{1}{2}, \frac{1}{2}$, respectively. The only crystallographic parameters are the temperature factors for each atom. Since the material is cubic these are isotropic.

0108-7673/88/030374-06$03.00

MgO has been studied extensively by X-ray and neutron methods. With neutrons only the reflections with even indices are observed. This is a consequence of both the closeness in scattering length for Mg and O and the near equality of the thermal parameters.

Togawa (1965), using a powder (grain size unspecified) and Cu $K\alpha$ radiation, found $B_{Mg} = 0{\cdot}24$, $B_O = 0{\cdot}19$ Å^2. Sanger (1969) used X-ray methods on a single crystal which had been irradiated to a neutron dose of 4×10^{20} n.v.t. At this dose interaction between dislocation loops leads to a substructure typical of an ideal mosaic crystal (Walker & Hickman, 1965). He obtained $B_{Mg} = 0{\cdot}346$ (9), $B_O = 0{\cdot}315$ (10) Å^2. Lawrence (1973) used a single crystal and Mo $K\alpha$ radiation. Only data collected at $(\sin\theta)/\lambda \geq 0{\cdot}5$ Å^{-1} were used. His result was $B_{Mg} = 0{\cdot}30$ (1), $B_O = 0{\cdot}34$ (2) Å^2. Beg (1976) used a fine powder, the grain size of which was estimated by Barron (1977) to be approximately 3 μm. He obtained a neutron powder pattern on a conventional neutron diffractometer equipped with an analyser for the removal of inelastically scattered neutrons. His value of the overall isotropic temperature factor was $B = 0{\cdot}354$ (8) Å^2. Barron (1977) considered the best thermodynamic value of the Debye temperature and obtained $B = 0{\cdot}3085$ (30) Å^2.

Two theoretical calculations have been made. Sanger (1969) carried out a lattice dynamical calculation based on the shell model, obtaining $B_{Mg} = 0{\cdot}287$, $B_O = 0{\cdot}350$ Å^2. Groenewegen & Huiszoon (1972) obtained $B_{Mg} = 0{\cdot}355$, $B_O = 0{\cdot}28$ Å^2 with a rigid ion model.

Barron (1977) concluded that the best estimate of B from a combination of all available data was $0{\cdot}314$ (10) Å^2.

3. Extinction

The only extinction mechanism which can operate in a powder is primary extinction. This depends on the size of each mosaic block. The equivalent of secondary extinction in powders is multiple scattering. In a random powder the mosaic block distribution function is known and the multiple scattering can, in principle, be calculated.

In an experiment multiple scattering is manifest as an apparent absorption. It can be distinguished from true absorption since multiple scattering augments the background to compensate for intensity removed from the Bragg peaks. True absorption removes intensity from both the Bragg and diffuse scattering.

Sabine (1988) has treated primary extinction using the Darwin intensity equations, the Bragg-case and Laue-case solutions to these equations, and a Lorentzian function for the coupling constant between the incident beam and the diffracted beam. The extinction coefficient E is defined by

$$I^{obs} = EI^{kin}. \tag{1}$$

I^{obs} is the integrated intensity observed in an experiment, I^{kin} is the integrated intensity calculated in the kinematic approximation. The notation E rather than the more usual y for the extinction factor is used to avoid any confusion with the powder-pattern ordinate. Then

$$E = E_L \cos^2\theta + E_B \sin^2\theta \tag{2}$$

$$E_L = 1 - x/2 + x^2/4 - 5x^3/48 + 7x^4/192 \qquad x \leq 1 \tag{3}$$

$$E_L = (2/\pi x)^{1/2}[1 - 1/8x - 3/128x^2 - 15/1024x^3] \qquad x > 1 \tag{4}$$

$$E_B = (1+x)^{-1/2} \tag{5}$$

$$x = (KN_c\lambda FD)^2. \tag{6}$$

In these expressions 2θ is the scattering angle, N_c is the number of unit cells per unit volume, λ is the wavelength, and F is the structure factor per unit cell (including the Debye–Waller factor) for the reflection under consideration. K is the shape factor. Its value is unity for a cube of edge D, 3/4 for a sphere of diameter D and $8/3\pi$ for a cylinder of diameter D.

When the specimen is composed of grains of unequal size, the extinction factors for each size are calculated from (2), (3), (4), (5) and (6), and are combined by the formula (Sabine, 1985)

$$E = \left(\sum_l f_l D_l^3\right)^{-1} \sum_l f_l D_l^3 E_l \tag{7}$$

to give a value of the extinction factor for the specimen.

E_l is the extinction factor for the grain size D_l; f_l is the fraction of such grains in the specimen.

4. The experiments

The specimens are described by Sabine (1985) and the same nomenclature will be used in this work. The grain size distributions and electron micrographs are given in that paper. The approximate average grain diameters were: *UM* 0·2, 2*M* 0·8, 4*M* 2, 20*M* 12, 50*M* 17 μm. The diffraction patterns were obtained on the Special Environment Powder Diffractometer (SEPD) at IPNS, Argonne National Laboratory, IL, USA. The axis of each cylinder was vertical and data were collected at nominal scattering angles of 150, 90 and 60°. All data were collected at room temperature.

5. Rietveld refinement

The computer program *GSAS* of Larson & Von Dreele (1986) was modified to use the extinction factor given by (2)–(6). The shape factor was taken as unity.

Table 1. *Parameters from GSAS refinement of the data from* MgO

All parameters shown with a standard deviation (given in parentheses after the value of the parameter) were refined.

Sample	*UM*	2*M*	20*M*	50*M*
Mass (g)	3·33	3·86	5·63	7·95
*N*150*	1491	1476	1468	1476
*N*90	862	856	853	854
R_{wp}, 150†	0·068	0·076	0·068	0·063
R_{wp}, 90	0·060	0·068	0·065	0·063
R_p, 150‡	0·045	0·051	0·046	0·043
R_p, 90	0·044	0·049	0·048	0·046
U (Å^2)	0·003910 (3)	0·00382 (3)	0·00404 (3)	0·00408 (3)
SG, 150§	10·50 (3)	9·51 (2)	19·79 (6)	21·57 (6)
SG, 90	6·99 (2)	6·31 (2)	12·96 (3)	13·38 (4)
DIFC, 150¶	7570·7 (4)	7568·4 (3)	7568·9 (3)	7569·7 (3)
DIFC, 90	5585·4 (4)	5586·1 (4)	5586·6 (3)	5585·9 (4)
DIFA, 150	−2·75 (18)	−2·57 (15)	−2·62 (16)	−2·32 (17)
DIFA, 90	−1·73 (18)	−0·65 (16)	−0·09 (16)	0·32 (18)
ZERO, 150	−7·07 (15)	−6·87 (13)	−7·02 (12)	7·26 (12)
ZERO, 90	−6·93 (19)	−6·76 (17)	−6·91 (16)	−6·77 (17)
ABS**	0·0217 (12)	0·0128 (11)	0·0366	0·0517
EXT (μm^2)**	0·0	0·0	75·4 (1·0)	140·2 (1·6)
AL1, 150††	0·22 (1)	0·310 (4)	0·330 (4)	0·380 (4)
AL1, 90	0·22 (1)	0·310 (4)	0·330 (4)	0·380 (4)
BE0, 150	0·0401 (2)	0·0412 (2)	0·0416 (2)	0·0412 (2)
BE0, 90	0·0401 (2)	0·0412 (2)	0·0416 (2)	0·0412 (2)
BE1, 150	0·00179 (2)	0·00184 (2)	0·00172 (2)	0·00455 (2)
BE1, 90	0·00480 (5)	0·00200 (4)	0·00441 (4)	0·00588 (4)
SG0, 150	3·07 (2)	2·9 (2)	2·3 (2)	2·7 (2)
SG0, 90	12·4 (4)	13·0 (3)	10·0 (3)	10·6 (4)
SG1, 150	13·0 (11)	18·5 (8)	19·6 (8)	26·9 (8)
SG1, 90	33·7 (16)	46·2 (12)	44·3 (12)	74·6 (14)
SG2, 150	15·4 (7)	3·9 (4)	1·9 (4)	2·4 (5)
SG2, 90	30·5 (9)	11·4 (6)	8·8 (6)	8·0 (7)

* N = number of profile data points used in refinement.
† $R_{wp} = \sum w_i(y_o - y_c)_i^2 / \sum w_i y_{oi}^2$.
‡ $R_p = \sum|(y_o - y_c)|/\sum y_o$.
§ SG = scale factor.
¶ DIFC, DIFA, ZERO = diffractometer constants.
** ABS = absorption parameter; EXT = extinction parameter.
†† AL1, BE0, BE1, SG0, SG1, SG2 = profile parameters.

After the modifications the value of the calculated ordinate for a single phase in a TOF powder pattern is given by

$$y(\lambda) = I(\lambda)[A(\lambda)S\sum L_k m_k F_k^2 G_k(\lambda) E_k(\lambda) + b], \quad (8)$$

where $A(\lambda)$ is the wavelength-dependent absorption correction for cylinders, and has been developed from the constant-wavelength expression of Hewat (1979). $I(\lambda)$ is the incident intensity. S is the scale factor. The sum is over k neighbouring reflections with multiplicity m_k, Lorentz factor L_k, structure factor (including the Debye–Waller factor) F_k, profile function G_k, extinction factor E_k.

The background, b is represented by a shifted Chebyschev polynomial of the first kind with refinable coefficients. The profile function is that of Von Dreele, Jorgensen & Windsor (1982) with modifications by Von Dreele (unpublished).

The data sets taken at the nominal scattering angles of 150 and 90° were included in the refinements of data from the *UM*, 2*M*, 20*M* and 50*M* specimens. The spectral coefficients for the incident intensity were those determined by Rotella (private communication) for the period over which the data were collected.

After a considerable number of exploratory refinements the final sequence of calculations proceeded by a refinement of a single absorption coefficient for the *UM* and 2*M* data with the extinction coefficient set to zero. While true absorption in MgO is negligible the effects of multiple scattering will be interpreted by the program as an apparent absorption factor.

The results are listed in the first two columns of Table 1. For the refinements of data from the 20*M* and 50*M* samples, the absorption coefficient was fixed at the value from the 2*M* refinement scaled by the ratio of the sample masses. The extinction coefficient was then refined with the other parameters. These results are listed as the remaining two columns in Table 1. Fig. 1 shows typical observed and calculated diffraction curves resulting from one of these refinements (50*M*).* The residual differences seen in

* Listings of the observed diffraction profiles at 90 and 150° (2θ) for samples U*M*, 2*M*, 20*M* and 50*M* have been deposited with the British Library Document Supply Centre as Supplementary Publication No. SUP44676 (72 pp.). Copies may be obtained through The Executive Secretary, International Union of Crystallography, 5 Abbey Square, Chester CH1 2HU, England.

these curves arise because the true peak shape is more complex than assumed in this analysis.

During the course of the calculations, a second set of peaks was noted in all of the 90° data sets. Apparently one detector tube in the 90° bank was incorrectly connected to the electronic recording system which caused additional reflections to appear. To compensate, a second phase of MgO with a larger lattice constant was included in the calculations for these detector banks; only the scale factor was refined for this phase.

For this investigation the refined quantities of particular interest are:

(1) EXT. This is the square of the edge length (D) of a cubic mosaic block. For $20M$, $D = 8{\cdot}7\,(1)$ μm and for $50M$, $D = 11{\cdot}8\,(1)$ μm.

(2) U. This is the overall temperature factor. $B = 8\pi^2 U$ and its value for the four specimens is, in units of Å^2, UM 0·309 (2), $2M$ 0·302 (2), $20M$ 0·319 (2), $50M$ 0·322 (2). The average value is 0·313 (10).

(3) SG2. This is a parameter in the profile function to allow for strain broadening. It can be seen that it is significantly greater in specimen UM. The reason for this is unknown. The strains may be produced during preparation and annealed by the heat treatment given to the other specimens.

6. Analysis of integrated intensities

As in the previous work (Sabine, 1985) the assumption was made that extinction was negligible in specimens UM, $2M$ and $4M$. The integrated intensity of the reflections from these specimens is then I^{kin} in (1).

If the number of atoms in each specimen was the same the experimental extinction factor for each reflection would be given by the ratio $I(hkl)$ for the $20M$ and $50M$ specimens to the mean $I(hkl)$ for UM, $2M$ and $4M$.

To correct for the fact that the number of atoms is not the same advantage was taken of the availability of data at very short wavelengths. As Marshall & Lovesey (1971) have shown the macroscopic scattering cross section in this energy region is the number of atoms multiplied by the scattering cross section of each atom. All interference effects have disappeared and the measured spectrum is directly proportional to the number of atoms in the specimen.

This procedure eliminates any errors in integrated intensity related to the position of the specimen in the beam, differences in the time taken for each run, and changes in the incident intensity. Since intensity ratios are taken for reflections at the same wavelength the experiment is also independent of the shape of the incident spectrum.

After normalization in this way it was found that the integrated intensities for $2M$ and $4M$ agreed to within 1%. However, the values for each reflection in UM were 10% lower. This effect, which had been noticed in the earlier work (Sabine, 1985), is attributed to the presence of very fine particles in this specimen. Because of extreme line broadening associated with these particles their contribution to the

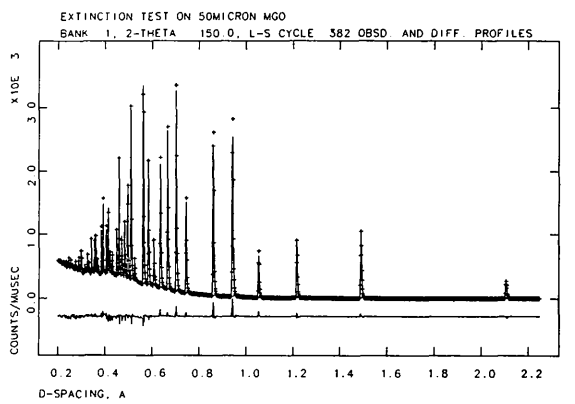

Fig. 1. Observed and calculated diffraction profiles for specimen $50M$.

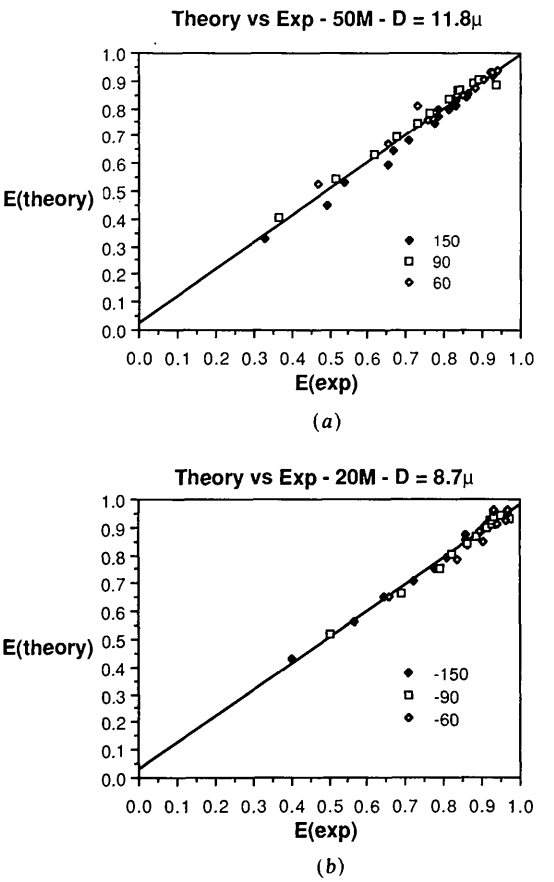

Fig. 2. (*a*) Effective mosaic block size obtained by Rietveld analysis fitted to the integrated intensity data from specimen $50M$. (*b*) Effective mosaic block size from Rietveld analysis fitted to integrated intensity data from specimen $20M$.

integrated intensity appeared as background. The fine particles, because of their high surface-area-to-volume ratio, were absorbed by the larger grains when the compacts were sintered to produce specimens of higher grain size. The influence of this effect in using neutron diffraction methods for the quantitative analysis of mixtures of powders has been demonstrated by Hill & Howard (1987). In this experiment the extinction-free values of the integrated intensity are taken as the mean of $2M$ and $4M$.

The results of the integrated intensity analysis are shown in Figs. 2(*a*) and (*b*). The experimental extinction factor E(exp.) was obtained by dividing the normalized integrated intensity for each reflection by the mean integrated intensity of the same reflection from $2M$ and $4M$. The three data sets (scattering angles 60, 90 and 150°) are included on the same graph. Each data point is a Bragg reflection.

The theoretical extinction factor for each grain size, E_i(exp.) was calculated from (1)–(6) using the mosaic block sizes given by Rietveld refinement. The overall temperature factor is taken as $B = 0{\cdot}314$ Å^2 and the scattering lengths as $b_{Mg} = 5{\cdot}375$ and $b_O = 5{\cdot}805$ fm (Koester & Yelon, 1982).

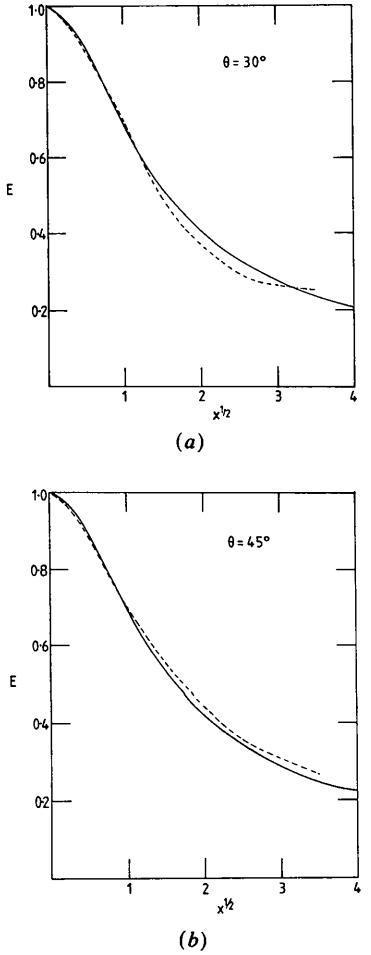

(*a*)

(*b*)

Fig. 3. A comparison of extinction corrections between the results of the present theory (full line), and the results of a dynamical theory prediction (broken line). (*a*) $2\theta = 60°$; (*b*) $2\theta = 90°$.

The agreement between theory and experiment shows that the refined value of the extinction parameter has physical significance. The single parameter D is not a simple average of the grain size in the specimen. However, the limiting values of extinction factor can be used to give it a meaning. As Sabine (1988) has shown, E_l becomes proportional to D_l^{-1} where D_l is the edge length of the block. Then, from (7),

$$1/D = \sum_l f_l D_l^2 \Big/ \sum_l f_l D_l^3.$$

7. Discussion

The extinction theory used in this paper is based on the Darwin–Hamilton intensity equations (Darwin, 1922; Hamilton, 1957). The dynamical theory of diffraction, which has a different starting point [see review by Werner, Berliner & Arif (1986)], has been used by Olekhnovich & Olekhnovich (1978) to calculate the primary extinction factor for the square-section parallelepiped. Their theory is not analytic and is limited to $2\theta \leq 90°$. However, they present results in a graphical form for $2\theta = 60$ and $2\theta = 90°$ which are scattering angles used in this experiment. Their parameter, τ, is equal to the square root of the parameter x of this paper.

A comparison of the predictions of both theories is given in Fig. 3. The dynamical theory result is taken from the published graphs. It can be seen that the results agree to a few percent and that, for the purpose of calculating the primary extinction factor, either starting point is acceptable.

8. Concluding remarks

It has been shown that the formulae given by Sabine (1988) predict the magnitude of primary extinction in finite crystals to a level at which the observed integrated intensity is one-third of the value expected from the kinematic approximation. These formulae, which are analytic and rapidly convergent, can be used in a least-squares refinement program for data collected at any scattering angle. If extinction is included Rietveld analysis of time-of-flight data gives meaningful values for the numerical values of temperature factors. This is particularly important in studies at high temperature, where grain growth will occur.

This work was carried out with the support of the Argonne National Laboratory, USA, the Rutherford–Appleton Laboratory, England and the Department of Energy, USA.

References

BARRON, T. H. K. (1977). *Acta Cryst.* A33, 602-604.
BEG, M. M. (1976). *Acta Cryst.* A32, 154-156.
DARWIN, C. G. (1922). *Philos. Mag.* 43, 800-829.
GROENEWEGEN, P. P. M. & HUISZOON, C. (1972). *Acta Cryst.* A28, 164-169.
HAMILTON, W. C. (1957). *Acta Cryst.* 10, 629-634.
HEWAT, A. W. (1979). *Acta Cryst.* A35, 248-249.
HILL, R. J. & HOWARD, C. J. (1987). *J. Appl. Cryst.* 20, 467-474.
HOWARD, C. J. & SABINE, T. M. (1974). *J. Phys. C*, 7, 3453-3465.
KOESTER, L. & YELON, W. B. (1982). *Summary of Low-Energy Neutron Scattering Lengths and Cross-Sections.* IUCr Commission on Neutron Diffraction.
LARSON, A. C. & VON DREELE, R. B. (1986). *GSAS - Generalised Crystal Structure Analysis System.* Los Alamos Report LAUR 86-748, Los Alamos National Laboratory, USA.
LAWRENCE, J. L. (1973). *Acta Cryst.* A29, 94-95.
MARSHALL, W. & LOVESEY, S. W. (1971). *Theory of Thermal Neutron Scattering.* Oxford: Clarendon Press.
OLEKHNOVICH, N. M. & OLEKHNOVICH, A. I. (1978). *Acta Cryst.* A34, 321-326.
RIETVELD, H. M. (1969). *J. Appl. Cryst.* 2, 65-71.
SABINE, T. M. (1985). *Aust. J. Phys.* 38, 507-518.
SABINE, T. M. (1988). *Acta Cryst.* A44, 368-373.
SANGER, P. L. (1969). *Acta Cryst.* A25, 694-702.
TOGAWA, S. (1965). *J. Phys. Soc. Jpn*, 20, 742-752.
VON DREELE, R. B., JORGENSEN, J. D. & WINDSOR, C. G. (1982). *J. Appl. Cryst.* 15, 581-589.
WALKER, D. G. & HICKMAN, B. S. (1965). *Philos. Mag.* 12, 445-451.
WERNER, S. A., BERLINER, R. R. & ARIF, M. (1986). *Physica (Utrecht)*, 137B, 245-255.

Acta Cryst. (1988). A44, 379-382

Combining Direct Methods with Isomorphous Replacement or Anomalous Scattering Data. VI. Incorporation of Heavy-Atom Information into Hauptman's Distributions*

BY HAO QUAN AND FAN HAI-FU

Institute of Physics, Academia Sinica, Beijing, China

(*Received* 23 *September* 1987; *accepted* 15 *January* 1988)

Abstract

Heavy-atom information has been incorporated into Hauptman's distributions of three-phase structure invariants for both isomorphous replacement and anomalous scattering cases. Reliable estimates of individual phases can be obtained by introducing the phase doublet expression $\varphi_H = \varphi'_H \pm |\Delta\varphi_H|$. A test calculation with error-free data of insulin showed results better than previous methods.

Introduction

In recent years, approaches based on the combination of direct methods with SIR (single isomorphous replacement) or OAS (one-wavelength anomalous scattering) have been well developed. Fan Hai-fu, Han Fu-son, Qian Jin-zi & Yao Jia-xing (1984) proposed that in the case of SIR or OAS the phase of a structure factor can be expressed as $\varphi_H = \varphi'_H \pm |\Delta\varphi_H|$, where φ'_H can be calculated from the heavy-atom sites and $|\Delta\varphi_H|$ can be derived from the experimental diffraction data. The phase problem is thus reduced to a matter of making a sign choice. Satisfactory estimates of individual phases were obtained by combining this phase-difference relation with Cochran's (1955) probability distribution. Hauptman (1982*a*, *b*) derived new probability distributions for threee-phase structure invariants in the SIR and OAS cases. The formulas proved to be more reliable than Cochran's distribution. However, there is still the potential to improve Hauptman's formulas by making use of heavy-atom information. In this context Fortier, Moore & Fraser (1985) obtained the full range (−1 to 1) of estimates of cosine invariants. However, the procedure yields a twofold ambiguity which would lead to difficulties in the derivation of individual phases. In this paper, improved Hauptman distributions are given, which make full use of the heavy-atom information. These distributions are then used instead of Cochran's distribution as the foundation of the individual phase derivation. The concept of 'best phase' (Fan Hai-fu, Han Fu-son & Qian Jin-zi, 1984) is also used for error treatment.

Theoretical basis

1. *The probability distribution of three-phase structure invariants*

According to Hauptman (1982*a*), there are four kinds of three-phase structure invariants in the SIR

* Part of this paper was presented at the International Symposium on Molecular Structure, Beijing, China, 15-19 September 1986.

0108-7673/88/030379-04$03.00